Food and Chemical Toxicology 134 (2019) 110835

Contents lists available at ScienceDirect

Food and Chemical Toxicology

journal homepage: www.elsevier.com/locate/foodchemtox

Carvacrol inhibits cadmium toxicity through combating against caspase dependent/independent apoptosis in PC12 cells

Subrata Banik[a], Mahmuda Akter[a], Serene Ezra Corpus Bondad[a], Takeshi Saito[b], Toshiyuki Hosokawa[c], Masaaki Kurasaki[a,d,*]

[a] Graduate School of Environmental Science, Hokkaido University, 060-0810, Sapporo, Japan
[b] Faculty of Health Sciences, Hokkaido University, 060-0812, Sapporo, Japan
[c] Institute for the Advancement of Higher Education, Hokkaido University, 060-0810, Sapporo, Japan
[d] Faculty of Environmental Earth Science, Hokkaido University, 060-0817, Sapporo, Japan

ARTICLE INFO

Keywords:
Food antioxidants
Oxidative stress
Glutathione
Pro-survival proteins
Cytochrome *c*
Apoptosis inducing factor

ABSTRACT

Carvacrol is a monoterpenic phenol found in essential oils, is considered a safe food additive, and possesses various therapeutic properties. Numerous studies have also deciphered the protective role of carvacrol on various cytotoxicities. We clarify the effects of carvacrol on cadmium-induced apoptosis in PC12 cells. Carvacrol while co-exposed with cadmium for 48 h raised PC12 cell viability in comparison to only cadmium exposed group. The co-exposure increased the cellular glutathione levels and promoted the expression of glutathione reductase. The magnitude of DNA fragmentation caused by cadmium was also ameliorated by carvacrol. Flow cytometry exhibited the apoptosis rate augmented by cadmium was reduced by carvacrol. Western blotting revealed that cadmium and carvacrol co-exposure alleviated the cadmium-induced down-regulations of mammalian target of rapamycin (mTOR), protein kinase B (Akt), nuclear factor kappa-light-chain-enhancer of activated B cells (NFKB), extracellular signal-regulated kinase-1 (ERK-1) and nuclear factor erythroid 2-related factor 2 (Nrf2) expressions. The co-exposure also reversed action of cadmium by suppressing the cleavage of caspase 3 and reducing the cytosolic levels of cytochrome *c* and apoptosis inducing factor (AIF). Moreover, carvacrol upon co-exposure significantly increased the intracellular metallothionein content. In conclusion, carvacrol strongly reduced cadmium-triggered oxidative stress and caspase-dependent and caspase-independent apoptosis in PC12 cells.

1. Introduction

Cadmium (Cd^{2+}), a heavy metal used in many industrial and household products, has become prioritized due to its emergence as a widespread environmental pollutant and a biological toxicant. Concern over Cd^{2+} is due to its extremely high toxicity, a long half-life in humans and being a causative agent for many diseases and disorders upon acute or chronic exposure (Järup and Åkesson, 2009; Jiang et al., 2014). Evidences support that Cd^{2+} exposure is associated with a variety of ailments including renal tubular dysfunction (Nishijo et al., 2006), osteoporosis (James and Meliker, 2013), hepatotoxicity (Dudley et al., 1982), cardiovascular diseases (Tellez-Plaza et al., 2013) and neurotoxicity (Wang and Du, 2013). Following absorption and distribution, Cd^{2+} affects cellular metabolic processes resulting to alterations in proliferation and differentiation. Cd^{2+} causes cellular injury through exerting oxidative stress (Patra et al., 2011), promoting DNA damage (Badisa et al., 2007), altering transport pathways (Kerkhove et al., 2010) and impairing mitochondrial membrane potential leading to apoptosis (Mao et al., 2011; Jiang et al., 2014). The landscape for Cd^{2+}-triggered death mechanisms have been studied extensively in various cell lines. However, the death mechanisms differ depending on cell type, Cd^{2+} concentration and duration of exposure. Despite many debates and complexities of mechanisms, previous reports detailed that *in vitro* cells frequently go through an apoptotic death at low to moderate (e.g., 0.1–10 μM) Cd^{2+} concentrations and undergo necrosis at high (> 50 μM) concentrations (Templeton and Liu, 2010). Numerous cell systems showed that diverse signaling pathways have been involved in Cd^{2+}-induced apoptosis including mitochondrial (Rahman et al., 2017), extrinsic (Liu et al., 2016a) and caspase-independent (Liu and Templeton, 2008) pathways. But, a rise in reactive oxygen species (ROS) levels, increased lipid peroxidation, alterations in antioxidant defense system, and stimulation of metallothionein formation are the

* Corresponding author. Faculty of Environmental Earth Science, Hokkaido University, Sapporo, 060-0810, Japan.
E-mail address: kura@ees.hokudai.ac.jp (M. Kurasaki).

https://doi.org/10.1016/j.fct.2019.110835
Received 10 August 2019; Received in revised form 19 September 2019; Accepted 21 September 2019
Available online 25 September 2019
0278-6915/

Abbreviations

AIF	apoptosis inducing factor
Akt	protein kinase B
ANOVA	single-factor analysis of variance
CVC	carvacrol
DTNB	5, 5′-dithiobis-2-nitrobenzoic acid
DTT	dithiothreitol
ECL	enhanced chemiluminescence
EGTA	ethylene glycol tetraacetic acid
ELISA	enzyme-linked immunosorbent assay
ERK-1	extracellular signal-regulated kinase-1
FBS	fetal bovine serum
GR	glutathione reductase
GSH	glutathione
HEPES	4-(2-hydroxyethyl)-1-piperazineethanesulfonic acid
HRP	horseradish peroxidase
LDH	lactate dehydorogenase
MT	metallothionein
mTOR	mammalian target of rapamycin
NaF	sodium fluoride
NFKB	nuclear factor kappa-light-chain-enhancer of activated B cells
Nrf2	nuclear factor erythroid 2-related factor 2
PBS	phosphate buffered saline
PCR	polymerase chain reaction
PMSF	phenylmethylsulfonyl fluoride
ROS	reactive oxygen species
SEM	standard error of mean

common phenomena cells follow upon Cd^{2+}-induced cytotoxicity, irrespective of apoptotic pathway(s) (Stohs et al., 2000; Sarkar et al., 1998).

Carvacrol (5-isopropyl-2-methyl-phenol) (CVC) is, a monoterpenoid phenol predominantly found as a natural constituent of various essential oils of *Labiateae* family plant species such as oregano, thyme and pepperwort (Noshy et al., 2018; Kirimer et al., 1995). It is generally considered as a food additive and flavoring agent (Zotti et al., 2013). Recently edible and non-edible CVC-based films have become very useful components in antimicrobial food packaging (Ramos et al., 2016). Numerous studies have reported the diverse biological and therapeutic properties of CVC including antimicrobial (Xu et al., 2008), antioxidant (Beena et al., 2013; Aristatile et al., 2009), anti-inflammatory (Landa et al., 2009), anti-carcinogenic (Karkabounas et al., 2006) and neuromodulatory (Zotti et al., 2013) activities. Cumulative evidences from *in vivo* and *in vitro* studies have already confirmed the protective role of CVC against various toxicant-induced oxidative stress and apoptosis in various organs and cell lines (Noshy et al., 2018; Aristatile et al., 2009; Wang et al., 2017; Samarghandian et al., 2016; Palabiyik et al., 2016). Another study also demonstrated that CVC can also alleviate Fe^{2+}-induced oxidative stress and apoptosis in SH-SY5Y cells (Cui et al., 2015). However, no report becomes available with regards to the potential protective effects of CVC on Cd^{2+}-induced toxicity in cell system with bio-molecular mechanistic clarifications.

Therefore, we hypothesized that CVC can induce protective effects against Cd^{2+}-induced cytotoxicity in cultured cells. Experiments were conducted to evaluate whether CVC has ameliorative effects against the cytotoxicity, oxidative stress and apoptosis caused by Cd^{2+} on PC12 cells. This study is assumed to be the first approach which would elucidate the abovementioned properties of CVC in a model cell line.

2. Materials and methods

2.1. Materials

PC12 cells were obtained from American Type Culture Collection (USA and Canada). Dulbecco's modified Eagle's medium (DMEM), ribonuclease A (RNase), ethidium bromide, and peroxidase-conjugated avidin were bought from Sigma (St. Louis, MO, USA). Fetal bovine serum (FBS) was purchased from Biosera (Kansas City, MO, USA). High pure polymerase chain reaction (PCR) product purification kit and proteinase K were acquired from Roche Diagnostics (Mannheim, Germany). Polyclonal antibodies against β-actin (cat# 4967), mammalian target of rapamycin (mTOR) (cat# 2972), cleaved caspase 3 (cat# 9661) and protein kinase B (Akt) (cat# 4691) were purchased from Cell Signaling Technology. Polyclonal antibodies against glutathione reductase (GR) (ab16801, Abcam), nuclear factor kappa-light-chain-enhancer of activated B cells (NFκB) (sc-109, Santa Cruz Biotechnology), extracellular signal-regulated kinase 1 (ERK1) (61003c, BD Transduction Laboratories), nuclear factor erythroid 2-related factor 2 (Nrf2) (PM069, MBL; Japan), caspase 3 (GTX110543, GeneTEX), and apoptosis inducing factor (AIF) (cat# 551429, BD Biosciences) were also procured. The Cytochrome *c* Release Apoptosis Kit (Q1A87-1KIT) was purchased from Calbiochem^{R}. Anti-mouse IgG (H + L) horseradish peroxidase (HRP) conjugate (W4021) and anti-rabbit IgG (H + L) horseradish peroxidase (HRP) conjugate (W4011) were bought from Promega Corporation (Madison, WI, USA). Enhanced chemiluminescence (ECL) western blotting detection reagent (Amersham Pharmacia Biotech., Buckinghamshire, England) and trypan blue (0.4%) solution (Bio-Rad, Hercules, CA, USA) were purchased. The AnnexinA5-FITC flowcytometry kit (cat# IM2375) was procured from Beckman Coulter (Marseille Cedex9, France) and metallothionein (MT) enzyme-linked immunosorbant assay (ELISA) kit (Lot# 160361) was collected from Frontier Science Co. Ltd. (Hokkaido, Japan). All other chemicals used were of analytical grade.

2.2. Cell culture and treatments

PC12 cells were cultured on 25 cm^2 cell culture flasks in DMEM supplemented with 10% fetal bovine serum (FBS) in a dehumidified incubator at 37 °C with 5% CO_2. After a 24 h pre-incubation, the cells were exposed to $CdCl_2$ (Cd^{2+}), or to CVC, or to both for 48 h. The exposure concentrations of CVC was first chosen as 0, 50, 100, 200 and 400 μM. But for further experimentation, the concentrations of Cd^{2+} and CVC used were selected as 10 μM and 100 μM, respectively.

2.3. Cell viability

Trypan blue exclusion test was used for the assessment of cell viability. PC12 cells were seeded at a density of about 1×10^5/flask and pre-incubated for 24 h until logarithmic growth phase was reached. The cells were then exposed with different concentrations of CVC (0, 50, 100, 200 and 400 μM) and Cd^{2+} (10 μM), separately; Co-exposure was done to cells using different non-toxic concentrations of CVC (0, 50, 100 and 200 μM) and Cd^{2+} (10 μM). After treatments and co-treatments, the cells were incubated for 48 h. Then, cells were subsequently collected and stained with 0.2% trypan blue in 1 × phosphate-buffered solution (PBS). The number of trypan blue-stained cells and total cells were counted using a cell counter (TC10™ Automated Cell Counter, Bio-Rad). Cell viability was expressed as percentage (%) of the trypan blue-stained cells.

2.4. Lactate dehydrogenase (LDH) activity assay

Cytotoxicity-derived cell membrane disintegration levels were assessed by measuring LDH activity in the cell treatment medium using a

nonradioactive cytotoxicity assay kit as described by Rahman et al. (2018). PC12 cells were exposed to Cd^{2+} (10 μM) or CVC (100 μM), or Cd^{2+} (10 μM) + CVC (100 μM) for 48 h. After exposure period, 50 μL of the culture medium was contained in a 1.5 mL tube and subsequently, 50 μL of substrate mixture (containing tetrazolium salts) was added to the tube. After incubating at room temperature for 30-min, 50 μL of stop solution was added. The absorbance at 490 nm was measured using an iMark™ microplate reader (BioRad; Hercules, CA, USA) to determine the amount of formazan dye produced. LDH activity was expressed as "LDH activity/1 × 10^6 cells". This experiment was repeated at least 3 times for ensuring biological and statistical reproducibility.

2.5. Measurement of intracellular glutathione (GSH) levels

Intracellular free-SH levels were determined following the methods previously described by Kihara et al. (2012) and Rahman et al. (2018). PC12 cells were harvested after 48 h exposure to Cd^{2+} (10 μM), CVC (100 μM) or Cd^{2+} (10 μM) + CVC (100 μM). The cells were then washed with 1 × PBS. A lysis buffer at an amount of 150 μL was added to the cells and incubated at room temperature for 10 min. Two freeze-thaw sonication cycles were executed in order to rupture the cell membranes. The resulting solution was centrifuged at 1500 rpm for 10 min to collect the supernatant. Then, the protein contents were measured spectrophotometrically using a protein assay dye reagent (Bio-Rad; Hercules, CA, USA). GSH levels were measured using 2.5 mM 5, 5′-dithiobis-2-nitrobenzoic acid (DTNB, pH 7). DTNB was added to the cell lysate at a concentration of 200 μM, and the absorbance at 412 nm was measured with a DU-65 spectrophotometer (Beckman, CA, USA). The free–SH concentration was determined by using a molecular coefficient factor of 13,600 per cell number (1 × 10^5). The experiments were conducted at least triplicate to achieve reproducibility.

2.6. Isolation of the genomic DNA

The genomic DNA of PC12 cells was isolated using high pure PCR template preparation kit following the manufacturer's instructions. After treatment with Cd^{2+} (10 μM), CVC (100 μM) or Cd^{2+} (10 μM) + CVC (100 μM) cells were incubated for 48 h. Then, the cells were harvested using a scraper, and centrifuged at 1500 rpm for 5 min to remove the supernatant. Afterwards, the cells were washed with 1 × PBS and centrifuged at 1500 rpm for 5 min. The procedure for isolation of the genomic DNA was then performed. The isolated DNA was incubated with RNase (10 μg/mL) for 15 min at 37 °C, followed by addition of 100% ethanol and 3M NaOAc buffer (pH 4.5) were added. The solution was allowed to stand overnight at −20 °C for DNA precipitation. The following day, precipitated DNA was centrifuged at 15,000 rpm for 7 min, and for another 3 min after being washed with 70% ethanol. The obtained DNA was dried and solved with 50 μL 1 × Tris/Borate/Ethylenediaminetetraacetic acid (TBE), followed by the measurement of DNA concentration using a GeneQuant (GE Heath Care; South East England, UK). Finally, DNA concentrations were equalized for all samples by adding 1 × TBE solution.

2.7. Agarose gel electrophoresis of genomic DNA

The extracted genomic DNA in PC12 cells was subjected to agarose gel electrophoresis to assess the fragmentation levels. DNA (5 μg) was mixed with loading dye and electrophoresed on a 1.5% agarose gel for 40 min at 100 V, using a submarine-type electrophoresis system (Mupid-ex, Advance, Tokyo, Japan). Following electrophoresis, the gel was soaked in ethidium bromide solution for 5–10 min. DNA fragmentation was visualized under UV illumination using a ChemiDoc XRS (Bio-Rad; Hercules, CA, USA). The fluorescence intensity of fragmented DNA was analyzed using a software named "Quantity One". The amount of intact DNA was expressed as the intensity ratio of the total DNA density to the fragmented DNA density. This experiment was repeated for at least three times to ensure reproducibility.

2.8. Detection of apoptosis rate by flow cytometry

The apoptosis rate of PC12 cells was detected by flow cytometric analysis. PC12 cells were harvested after 48 h exposure to 10 μM Cd^{2+}, 100 μM CVC or to combined 10 μM Cd^{2+} and 100 μM CVC. Then cells were washed with 1 × PBS and 400 μL ice-cold 1 × binding buffer was subsequently added to the cells. Afterwards, 5 μL of annexin A5-FITC solution and 2.5 μL of propidium iodide (PI) were added to the cells and the resulting solution was kept for 10 min in the dark. Finally, samples were analyzed using a BD FACSVerse™ Flowcytometer. The experiment was conducted at least in triplicates for biological and statistical reproducibility.

2.9. Western blot analysis for the determination of protein expressions

Western blot analysis was accomplished for the determination of protein expressions in PC12 cells 48 h after exposure to the aforementioned Cd^{2+} and/or CVC concentrations. Cells were harvested and washed by suspending in ice-cold 1 × PBS, then centrifuged at 1500 rpm for 10 min. After removing the supernatant the cells were re-suspended in 150 μL of lysis buffer (consisting of 2 mM 4-(2-hydroxyethyl)-1-piperazineethanesulfonic acid (HEPES), 100 mM NaCl, 10 mM ethylene glycol tetraacetic acid (EGTA), 0.1 mM phenylmethylsulfonyl fluoride (PMSF), 1 mM Na_3VO_4, 0.1 mM Na_2MoO_4, 5 mM 2-glycerophosphorate, 10 mM $MgCl_2$, 2 mM dithiothreitol (DTT), 50 mM sodium fluoride (NaF), and 1% Triton X-100) for total protein extraction. The mixture was allowed to stand on ice for 10 min and then cells were disrupted by two cycles of sonication followed by centrifugation at 1500 rpm for 10 min to collect the lysate containing the total cellular protein. On the other hand, the cytosolic protein fractions were extracted using the cytosolic lysis buffer provided in the 'cytochrome *c* release apoptosis kit (Q1A87-1KIT)'. The concentration of extracted protein in the lysates was determined spectrophotometrically using a protein assay dye reagent (BioRad, Hercules, CA, USA). Thereafter, an equal amount (20 μg) of each protein sample was separated by 12.5–15% sodium dodecyl sulfate-polyacrylamide gel electrophoresis (SDS-PAGE). The electrophoresed proteins were then transferred into a nitrocellulose membrane using a semi-dry blotting system (type- AE6678; ATTO, Tokyo, Japan). The membranes were incubated overnight at 4 °C in 5% skimmed milk as a blocking agent. After blocking, each membrane was washed three times with 0.1% Tween buffer and incubated with the desired primary and secondary antibodies. After washing with 0.1% Tween buffer, the protein band on the nitrocellulose membrane was visualized using enhanced chemiluminescence, and analyzed using a ChemiDoc XRS (Bio-Rad, USA). Finally, the band intensities of the targeted proteins were expressed as the ratio to the intensity of β-actin. Each experiment was conducted at least in triplicates to ensure reproducibility.

2.10. Intracellular, Cd^{2+} accumulation in PC12 cells

The PC12 cells were incubated for 48 h after being exposed to 10 μM Cd^{2+} and/or 100 μM CVC. Following harvesting and washing with 1 × PBS cells were digested with 1 M nitric acid at 70 °C for 1 h. Then, the digested samples were filtered through a 0.22 μM pore membrane and diluted using deionized water to prepare for measurement. Intracellular cadmium contents were measured by using an ICPE-9000 inductively coupled plasma mass spectrometry (ICP-MS) (Shimadzu; Kyoto, Japan). To confirm the reproducibility, this experiment was carried out in triplicate.

2.11. Determination of metallothionein (MT) content

PC12 cells were exposed to 10 μM Cd^{2+} and/or 100 μM CVC for 48 h, harvested, and washed twice with 1 × PBS. The protein from the cells was extracted and the total protein content was measured spectrophotometrically using a protein assay dye reagent (Bio-Rad, Hercules, CA USA). The MT content in the cell lysate was measured by ELISA kit following manufacturer's protocol. The provided 96 well microtiter plate was first washed with PBS solution followed by the addition of 50 μL of standard or sample solution in each well. After adding 50 μL first antibody in each well, the microtiter plate was incubated at room temperature for 1 h. Then, each of the wells was washed thrice with 350 μL washing buffer and afterwards, 100 μL of second antibody was added. Following 1 h incubation at room temperature wells were washed and 100 μL of substrate mixture was subsequently added to each well while keeping the set-up in the dark. The reaction was stopped by adding 50 μL of stop solution. Finally, absorbance of the solution was measured at 450 nm in an ELISA reader (ng/mg of protein) and the concentration was calculated from a standard curve of MT protein.

2.12. Statistical analysis

Data were represented as the mean ± standard error of mean (SEM); $p < 0.05$ was considered to indicate significance level. Analysis of statistical significance was achieved by using single-factor analysis of variance (ANOVA) followed by unpaired Student's t-test in MS Excel 2013 program.

3. Results

3.1. Effects of Cd^{2+} and CVC on the viability of PC12 cells

To investigate the toxicity of CVC, PC12 cells were exposed to 50, 100, 200 and 400 μM of CVC for 48 h. Cells were also exposed to 10 μM of Cd^{2+} and combined Cd^{2+} and CVC. Trypan blue staining method was performed to assess the viability of PC12 cells. The results showed that the treatments of CVC up-to 200 μM did not affect the cell viability (Fig. 1A), indicating that the CVC concentrations used in this study were not toxic. On the other hand, the decrease in the PC12 cell viability caused by 10 μM Cd^{2+} was significantly ($p < 0.05$) prevented by CVC (100 or 200 μM) (Fig. 1B). Therefore, it was proposed from the cell viability results that CVC (100 or 200 μM) exerted cytoprotective effects against Cd^{2+} (10 μM)-induced cell death. The results were used as basis of choosing 10 μM Cd^{2+} and 100 μM CVC for further experimentation.

3.2. CVC reduces Cd^{2+} induced-LDH leakage

The soluble cytosolic enzyme LDH released in the cell culture media upon plasma membrane disintegration is one of the important indicators of toxicant-induced cell death. The LDH activity was measured in PC12 cell culture media after 48 h exposure to Cd^{2+} (10 μM) and/or CVC (100 μM). As shown in Fig. 2, compared to the control, Cd^{2+} (10 μM) exposure noticeably ($p < 0.05$) increased the LDH activity in

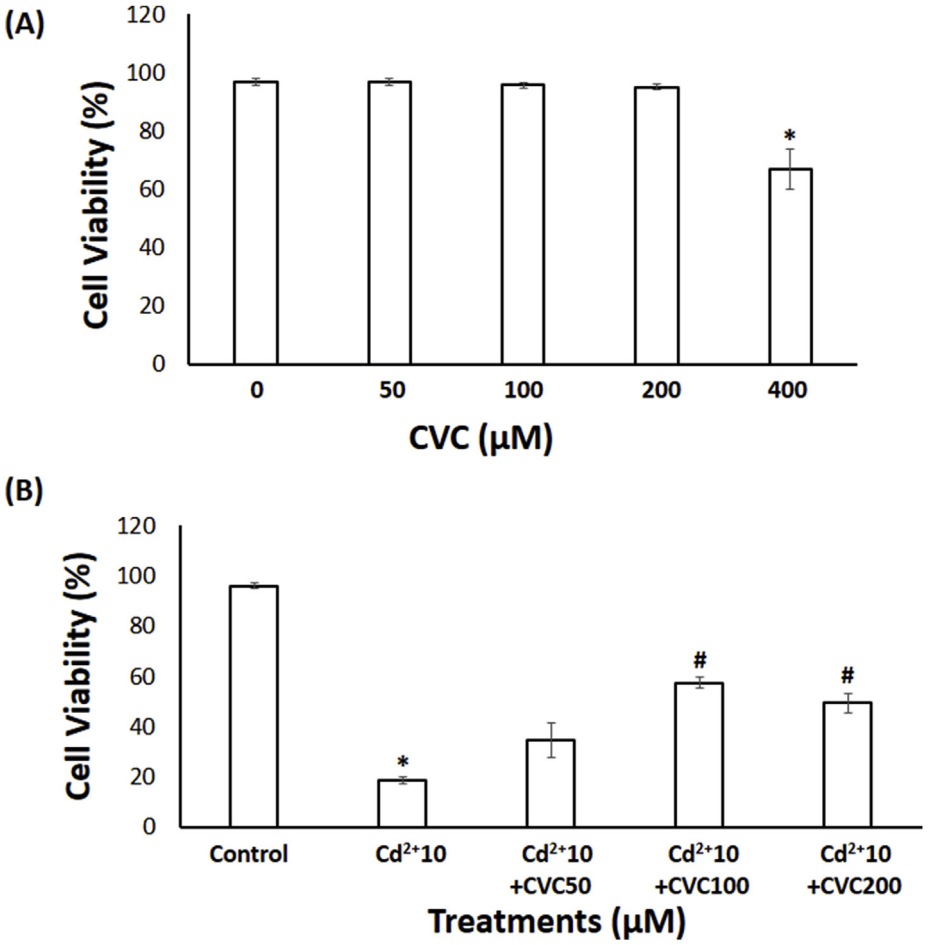

Fig. 1. Viability (%) of PC12 cells using trypan blue exclusion method. (A) PC12 cells exposed with 50, 100, 200 and 400 μM CVC for 48 h. (B) PC12 cells exposed/co-exposed with 10 μM Cd^{2+} and 50, 100, and 200 μM CVC for 48 h. Error bars indicate mean ± S.E.M. (n = 4 for (A) and 3 for (B)), * and # indicate significant differences ($P < 0.05$) from the control group and the Cd^{2+}-exposed group respectively.

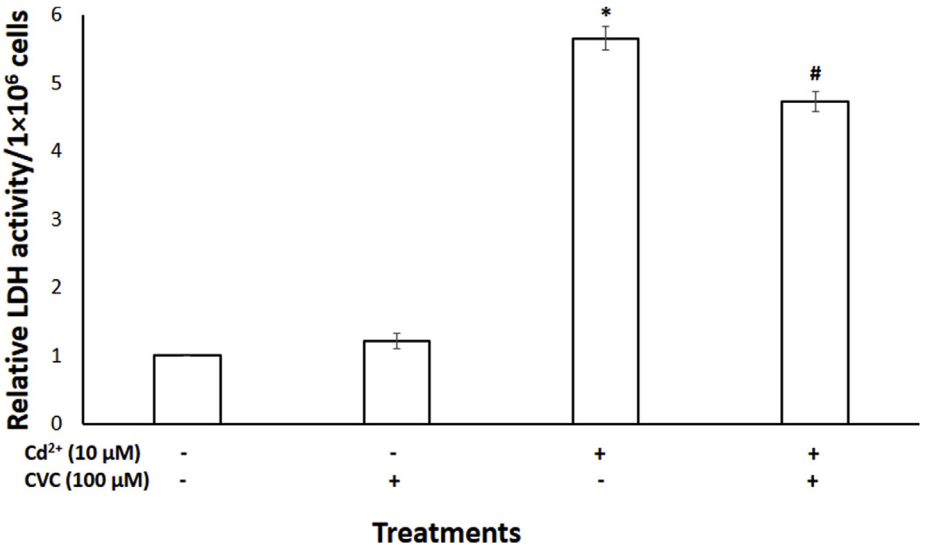

Fig. 2. LDH activity in the culture medium of PC12 cells exposed/co-exposed with 10 μM Cd^{2+} and 100 μM CVC for 48 h measured by a non-radioactive cytotoxicity assay kit. Error bars indicate mean ± S.E.M. (n = 3), * and # indicate significant differences ($P < 0.05$) from the control group and the Cd^{2+}-exposed group respectively.

the culture medium. On the other hand, no significant change in LDH activity was observed 48 h after CVC (100 μM) exposure. The combined exposure of Cd^{2+} (10 μM) and CVC (100 μM) significantly ($p < 0.05$) reduced the LDH activity in the medium compared to that only Cd^{2+} (10 μM) exposed group.

3.3. Effects of Cd^{2+} and CVC on the intracellular GSH levels and GR expression

GSH is the most abundant intracellular non-protein thiol which acts as an antioxidative defense system and removes oxidative stress generating electrophiles to maintain the redox homeostasis (Du et al., 2009). We exposed PC12 cells to Cd^{2+} (10 μM) and/or CVC (100 μM) for 48 h, and then measured intracellular GSH levels. A significant ($p < 0.05$) decrease in intracellular GSH content was found in the cells exposed to Cd^{2+} (10 μM), which was markedly ($p < 0.05$) increased in the cells with combined Cd^{2+} (10 μM) and CVC (100 μM) (Fig. 3A). However, no change in GSH level was found in cells exposed to CVC (100 μM) only. Thus, it can be suggested that CVC ameliorated oxidative stress posed by Cd^{2+} in PC12 cells. Additionally, Western blot analysis showed that expression of GR, the enzyme converting GSSG to GSH, supported the results found for GSH levels (Fig. 3B). Therefore, CVC showed antagonizing role on Cd^{2+}-induced oxidative damage.

3.4. CVC alleviates Cd^{2+}-induced genomic DNA damage

Genomic DNA damage is one of the major biological outcome of cadmium toxicity and is also a prominent route of cell inactivation in apoptosis (Roos and Kaina, 2006). In this study, agarose gel electrophoresis results exhibited that the amount of intact genomic DNA in PC12 cells was severely diminished after 48 h of Cd^{2+} (10 μM) exposure (Fig. 4A). On the other hand, it became visible that the exposure to CVC (100 μM) had no effect on the amount of intact genomic DNA compared to that of the untreated control cells. Cd^{2+} (10 μM)-induced DNA fragmentation was lessened in the case of cells exposed to combined Cd^{2+} (10 μM) and CVC (100 μM). In the line with this, we found a significant decrease in DNA band density in Cd^{2+} (10 μM) exposed cells, while the DNA band density for cells co-exposed with Cd^{2+} (10 μM) and CVC (100 μM) was markedly ($p < 0.05$) higher in comparison to only Cd^{2+} (10 μM) treated group (Fig. 4B). Thus, the co-exposed cell group possessed a comparatively reduced DNA damage.

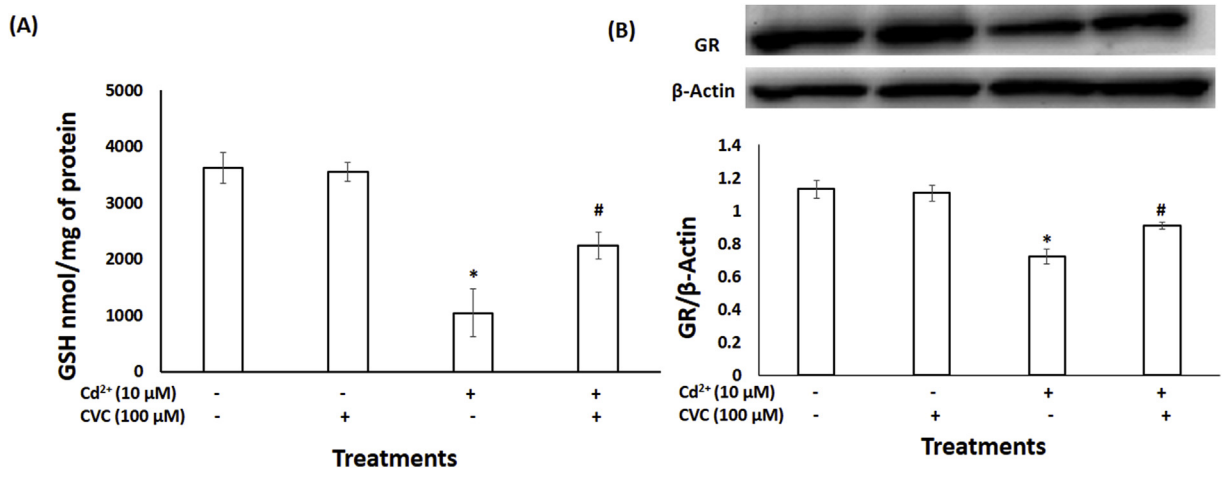

Fig. 3. Oxidative stress markers in PC12 cells exposed/co-exposed with Cd^{2+} and CVC. (A) Intracellular glutathione (GSH) level in PC12 cells exposed/co-exposed with 10 μM Cd^{2+} and 100 μM CVC for 48 h measured using DTNB. (B) GR expressed in PC12 cells exposed/co-exposed with 10 μM Cd^{2+} and 100 μM CVC for 48 h analyzed by western blotting. Error bars indicate mean ± S.E.M. (n = 4), * and # indicate significant differences ($P < 0.05$) from the control group and the Cd^{2+}-exposed group respectively.

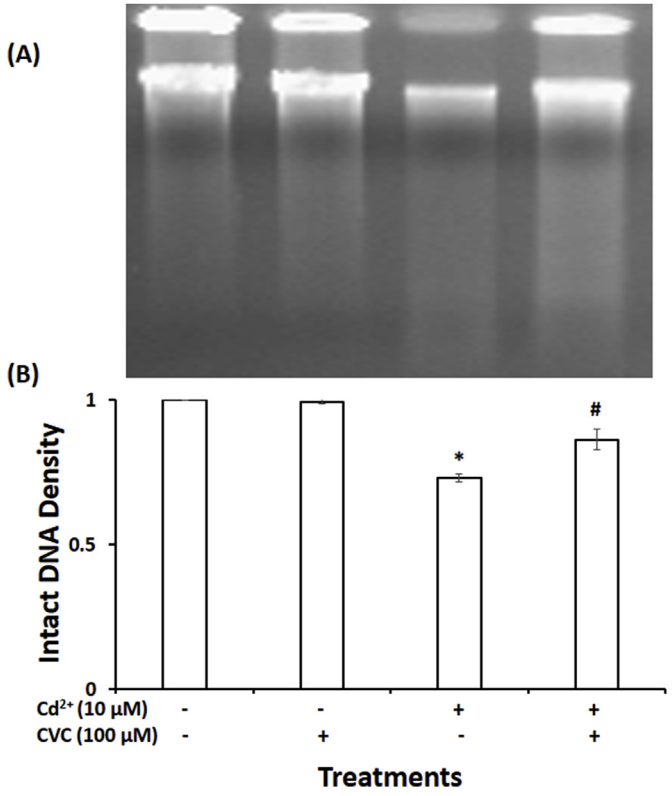

Fig. 4. Agarose gel electrophoresis of genomic DNA extracted from PC12 cells exposed/co-exposed with 10 μM Cd^{2+} and 100 μM CVC for 48 h. (A) A sample electrophoresis image showing the content of intact and fragmented genomic DNA of PC12 cells exposed/co-exposed with Cd^{2+} and CVC. (B) Relative band intensity of intact DNA for fragmentation detection. Error bars indicate mean ± S.E.M. (n = 3), * and # indicate significant differences ($P < 0.05$) from the control group and the Cd^{2+}-exposed group respectively.

3.5. CVC decreases the rate of Cd^{2+} induced apoptosis in PC12 cells

To determine the rate of apoptosis, PC12 cells were exposed to Cd^{2+} (10 μM) and/or CVC (100 μM) for 48 h. Then, the apoptotic rate was determined by annexin-V-FITC/PI assay using flow cytometry analysis (Fig. 5A). As shown in Fig. 5B, more than 54% of the Cd^{2+} (10 μM) exposed cells were in either early (in lower left (LL) quadrant) or late (in upper right (UR) quadrant) apoptotic condition. Although only CVC (100 μM) exposure did not change the apoptosis rate compared to that of the control group (4.65%), Cd^{2+} (10 μM) and CVC (100 μM) co-exposure markedly ($p < 0.05$) diminished the apoptosis rate to about 26%. These results suggest that CVC strongly reduced Cd^{2+}-provoked apoptosis in PC12 cells.

3.6. Effects of Cd^{2+} and CVC on the expressions of pro-survival proteins

We analyzed the expression of protein factors crucial for cell metabolism, proliferation, and survival in PC12 cells after exposure to Cd^{2+} (10 μM), or CVC (100 μM), or co-exposing with both Cd^{2+} (10 μM) and CVC (100 μM). The Western blot analyses images for the expressions of mTOR, Akt and NFκB were shown in Fig. 6A. Results exhibited that only Cd^{2+} (10 μM) exposure significantly ($p < 0.05$) down-regulated the expressions of mTOR, Akt and NFκB in comparison to the control. Compared to Cd^{2+} (10 μM) exposed group, all of these pro-survival proteins were evidently ($p < 0.05$) up-regulated in PC12 cells co-exposed to Cd^{2+} (10 μM) and CVC (100 μM) (Fig. 6B). Thus, the above results support that CVC (100 μM) could enhance the survival rate and protect PC12 cells from Cd^{2+} (10 μM)-induced oxidative stress and apoptosis.

3.7. CVC enhances the expressions of ERK1 and Nrf2 suppressed by Cd^{2+}

ERK1, a member of mitogen-activated protein kinase (MAPK) protein family, is generally considered as a regulator of many pro-survival and anti-apoptotic proteins. On the other hand, Nrf2 is a transcription factor that regulates the expressions of many antioxidant enzymes. In Fig. 7A, the representative Western blot images of the expressions of ERK1 and Nrf2 in PC12 cells showed that the expressions of both ERK1

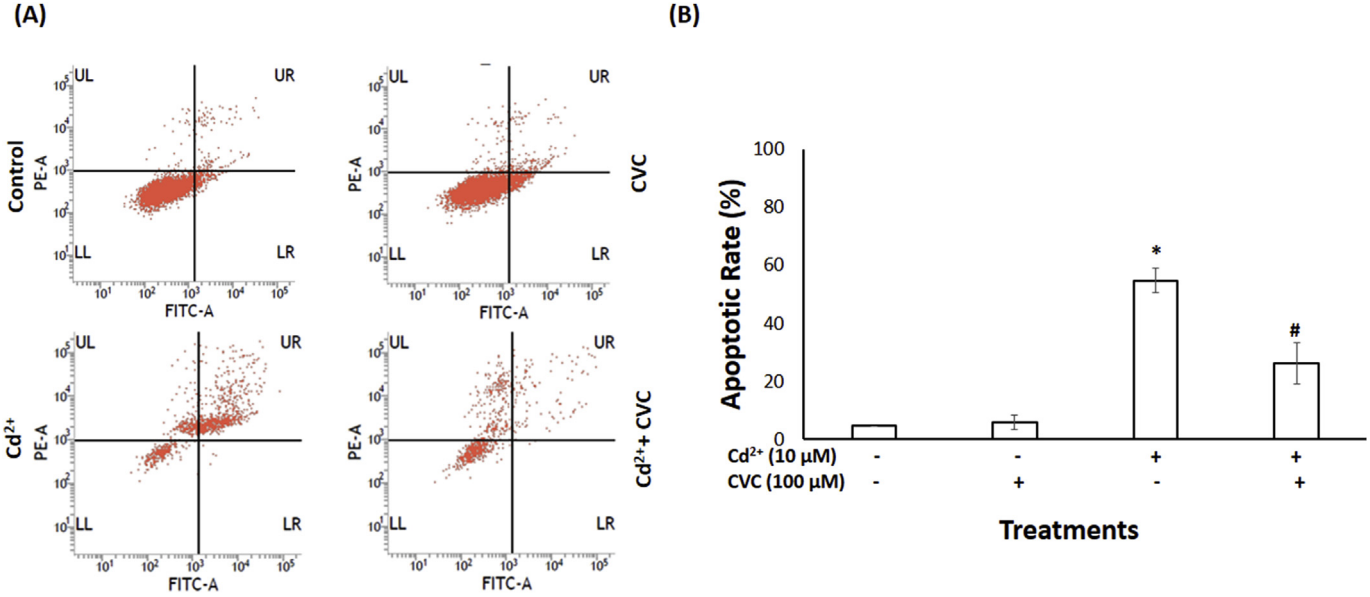

Fig. 5. The apoptotic rate of PC12 cells exposed/co-exposed with 10 μM Cd^{2+} and 100 μM CVC for 48 h analyzed by flow cytometry. (A) A representative experimental result of flow cytometry followed by annexin V-fluorescein isothiocyanate (FITC) and PI staining of PC12 cells exposed/co-exposed with Cd^{2+} and CVC for 48 h. (B) The apoptotic rate of PC12 cells exposed/co-exposed with Cd^{2+} and CVC for 48 h, calculated and analyzed using early apoptosis (LR) and late apoptosis (UR). Error bars indicate mean ± S.E.M. (n = 3), * and # indicate significant differences ($P < 0.05$) from the control group and the Cd^{2+}-exposed group respectively.

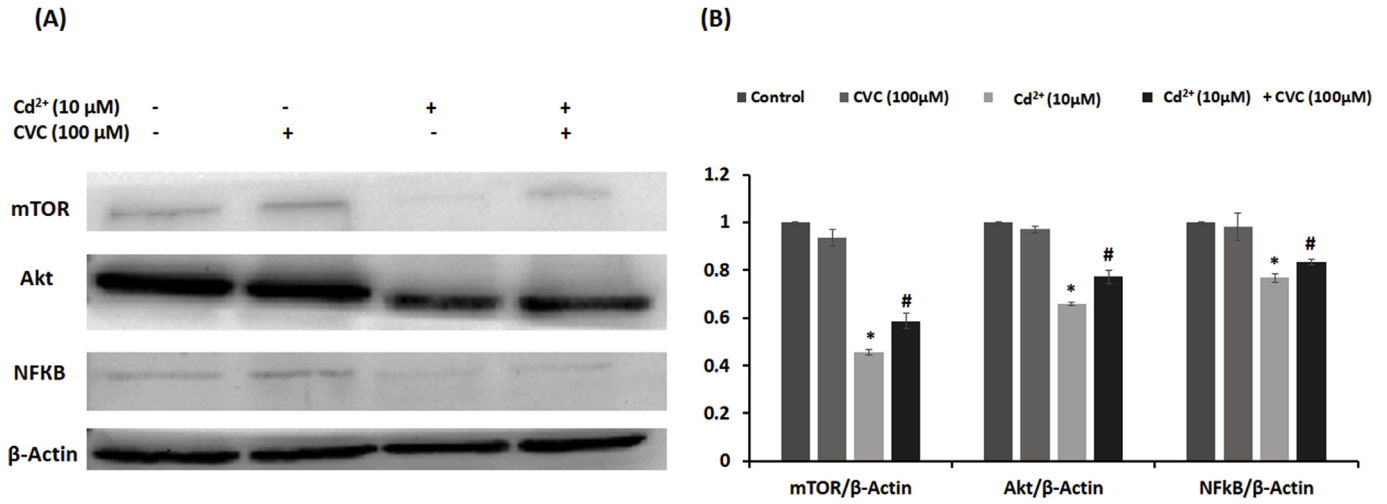

Fig. 6. Western blot analysis for the expression of pro-survival proteins in PC12 cells exposed/co-exposed with 10 μM Cd^{2+} and 100 μM CVC for 48 h. (A) The representative images (cropped) of immunoblotting for the expressions of mTOR, Akt and NFκB in PC12 cells exposed/co-exposed with Cd^{2+} and CVC for 48 h. (B) Relative density for the expression bands of mTOR, Akt and NFκB to β-actin in PC12 cells exposed/co-exposed with Cd^{2+} and CVC for 48 h. Error bars indicate mean ± S.E.M. (n = 3), * and # indicate significant differences (P < 0.05) from the control group and the Cd^{2+}-exposed group respectively.

and Nrf2 became significantly ($p < 0.05$) lessened due to the exposure to Cd^{2+} (10 μM) for 48 h. But, the band for co-exposed group was much more visible. The quantified expression levels of ERK1 and Nrf2 represented in Fig. 7B imply that upon co-exposure CVC (100 μM) significantly ($p < 0.05$) alleviated the Cd^{2+} (10 μM)-induced reduction of ERK1 and Nrf2 protein expressions.

3.8. Effects of CVC on Cd^{2+}-induced cleavage of caspase 3

The activation of caspase 3 by cleavage is the final event in the caspase cascade reactions in apoptotic cellular execution. PC12 cells were exposed to Cd^{2+} (10 μM), or CVC (100 μM), or both Cd^{2+} (10 μM) and CVC (100 μM) for 48 h. We found a substantial ($p < 0.05$) uplift in cleaved caspase 3 level in Cd^{2+} (10 μM) exposed cell group. Whereas, this level of cleaved caspase 3 was found to be lowered in cells exposed to combined Cd^{2+} (10 μM) and CVC (100 μM) (Fig. 8A and B). On the other hand, the expression of caspase 3 in Cd^{2+} (10 μM) exposed cells became down-regulated significantly but showed no difference with co-exposed cell group. Therefore, from the results it was ascertain that CVC saves PC12 cells from Cd^{2+} (10 μM)-induced apoptosis by hindering the cleavage of caspase 3.

3.9. Effects of CVC on Cd^{2+}-induced release of cytochrome c and AIF from mitochondria into the cytosol

The release of the hallmark protein cytochrome *c*, from the mitochondria into the cytosol, is essential to initiate the caspase cascade reaction leading to apoptosis. On the other hand, the mitochondrial membrane protein, AIF takes part in chromatin condensation and DNA fragmentation; and is translocated to the nucleus via cytosol during apoptosis. The results show a significant ($p < 0.05$) increase in cytosolic cytochrome *c* and AIF after exposing PC12 cells with Cd^{2+} (10 μM), which became considerably ($p < 0.05$) lesser for Cd^{2+} (10 μM) and CVC (100 μM) co-exposed groups (Fig. 9A and B).

3.10. Effects of CVC on Cd^{2+} uptake and MT expressions in PC12 cells

After exposing cells to Cd^{2+} (10 μM) and/or CVC (100 μM) for 48 h, the Cd^{2+} uptake by PC12 cells was measured using an ICP-MS. Although not significant, the Cd^{2+} uptake was higher in cells co-exposed to Cd^{2+} (10 μM) and CVC (100 μM) (Fig. 10) in comparison to cells exposed to Cd^{2+} (10 μM) only. Furthermore, we measured the MT expressions in the cells to explain the phenomenon of Cd^{2+} uptake increase in the co-exposed group. Fig. 11 shows that the expression of

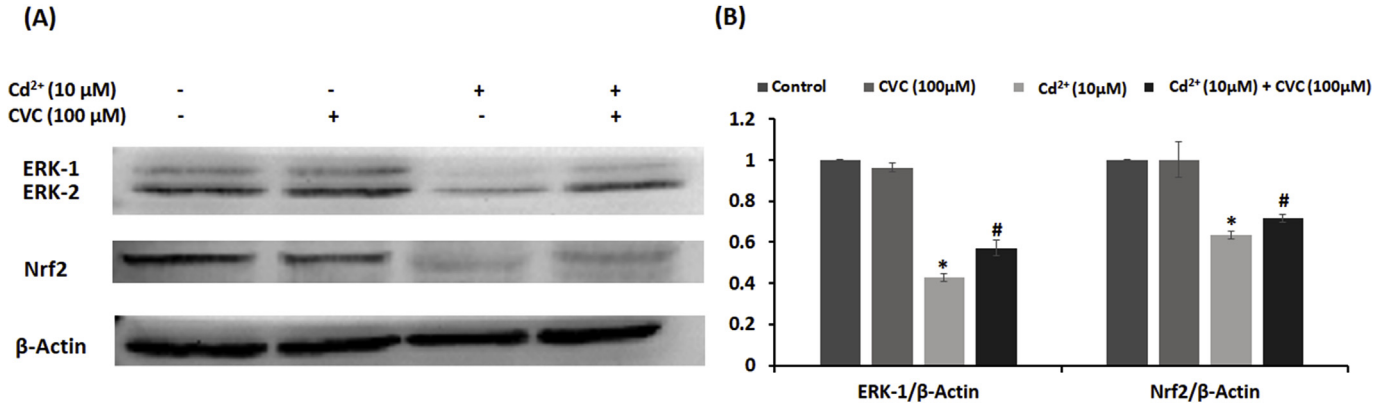

Fig. 7. Western blot analysis for the expression of ERK-1 and Nrf2 in PC12 cells exposed/co-exposed with 10 μM Cd^{2+} and 100 μM CVC for 48 h. (A) The representative images (cropped) of immunoblotting for the expressions of ERK-1 and Nrf2 in PC12 cells exposed/co-exposed with Cd^{2+} and CVC for 48 h. (B) Relative density for the expression bands of ERK-1 and Nrf2 to β-actin in PC12 cells exposed/co-exposed with Cd^{2+} and CVC for 48 h. Error bars indicate mean ± S.E.M. (n = 3), * and # indicate significant differences (P < 0.05) from the control group and the Cd^{2+}-exposed group respectively.

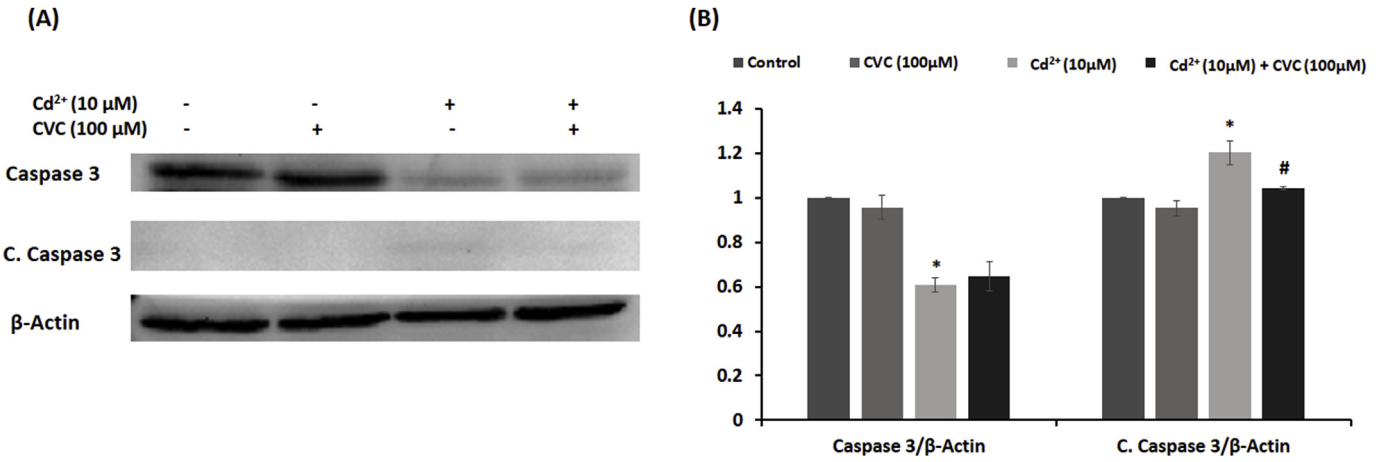

Fig. 8. Western blot analysis for the expression of caspase 3 and cleaved caspase 3 (c. caspase 3) in PC12 cells exposed/co-exposed with 10 μM Cd^{2+} and 100 μM CVC for 48 h. (A) The representative images (cropped) of immunoblotting for the expressions of caspase 3 and c. caspase 3 in PC12 cells exposed/co-exposed with Cd^{2+} and CVC for 48 h. (B) Relative density for the expression bands of caspase 3 and c. caspase 3 to β-actin in PC12 cells exposed/co-exposed with Cd^{2+} and CVC for 48 h. Error bars indicate mean ± S.E.M. (n = 3), * and # indicate significant differences ($P < 0.05$) from the control group and the Cd^{2+}-exposed group respectively.

MT was significantly increased in co-exposed cells in comparison to only Cd^{2+} (10 μM) exposed cells. Thus, the results indicate that upon co-exposure, CVC increased the MT expressions in PC12 cells which increased the Cd^{2+} uptake by MT binding.

4. Discussion

In recent times, natural antioxidants have been attentively examined since these can act as potential preventive mechanism against many toxicants to humans. In line with this, CVC, a food component possessing strong antioxidant activity, is believed to be a promising candidate (Aeschbach et al., 1994). Therefore, the objectives of this study were to define the roles of CVC on Cd^{2+}-induced cytotoxicity and to interpret the mechanisms behind those roles through cellular and molecular perspectives. In this study, it was found that CVC effectively lessens the immensity of Cd^{2+}-induced oxidative stress and apoptosis in PC12 cells. We also elucidated the underlying molecular mechanisms involved in the prevention of Cd^{2+}-induced toxicity in PC12 cells for the first time.

Numerous studies in a variety of cell lines suggest that Cd^{2+} toxicity is often associated with oxidative stress due to the over-generation of ROS causing cell-cycle degradation, deterioration of biological macromolecules and ultimately leading to apoptosis (Hu et al., 2015; Oh and Lim, 2006; Zhou et al., 2009; Chatterjee et al., 2009). In mammalian cells GSH plays a key role in combating ROS. ROS also interacts with classical antioxidant enzymes such as superoxide dismutase (SOD), catalase (CAT), glutathione peroxidase (GPx) and GR. The efficiency of GSH to regenerate depends on the redox state of the glutathione disulphide-glutathione couple (GSSG/2GSH) (Nemmiche, 2017). In line with this, the rate of the conversion of GSSG to GSH depends on the efficiency of the key enzyme GR. In this study, upon treatments and co-treatments, the intracellular GSH levels and the expressions of GR in PC12 cells were determined as oxidative stress markers (Fig. 3A and B). The results in our research demonstrated that Cd^{2+} (10 μM) exposure negatively affected the levels of both markers. Thus, our results were in agreement with the results found in other cell lines such as CRL-1439 normal rat liver cells (Ikediobi et al., 2004). On the other hand, CVC (100 μM) significantly boosted GSH and GR levels upon co-exposure with Cd^{2+} (10 μM). Thus, CVC saves PC12 cells from Cd^{2+}-induced oxidative stress by replenishing two vital components of antioxidant defense mechanisms; the low-molecular weight thiol compound, GSH and the enzyme reducing GSSG to GSH, GR. Our results also exhibited that the acute oxidative stress posed by Cd^{2+} (10 μM) exposure for 48 h also caused the significant number of PC12 cell death

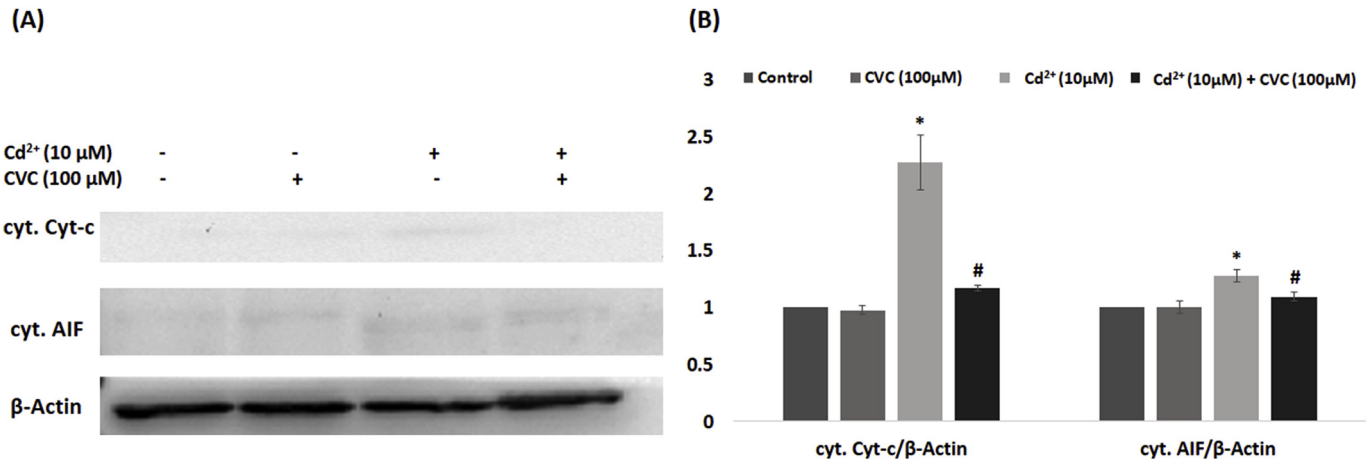

Fig. 9. Western blot analysis for cytosolic cytochrome *c* (cyt. Cyt-c) and cytosolic AIF (cyt. AIF) in PC12 cells exposed/co-exposed with 10 μM Cd^{2+} and 100 μM CVC for 48 h. (A) The representative images (cropped) of immunoblotting for cyt. Cyt-c and cyt. AIF in PC12 cells exposed/co-exposed with Cd^{2+} and CVC for 48 h. (B) Relative density for cyt. Cyt-c and cyt. AIF to β-actin in PC12 cells exposed/co-exposed with Cd^{2+} and CVC for 48 h. Error bars indicate mean ± S.E.M. (n = 3), * and # indicate significant differences ($P < 0.05$) from the control group and the Cd^{2+}-exposed group, respectively.

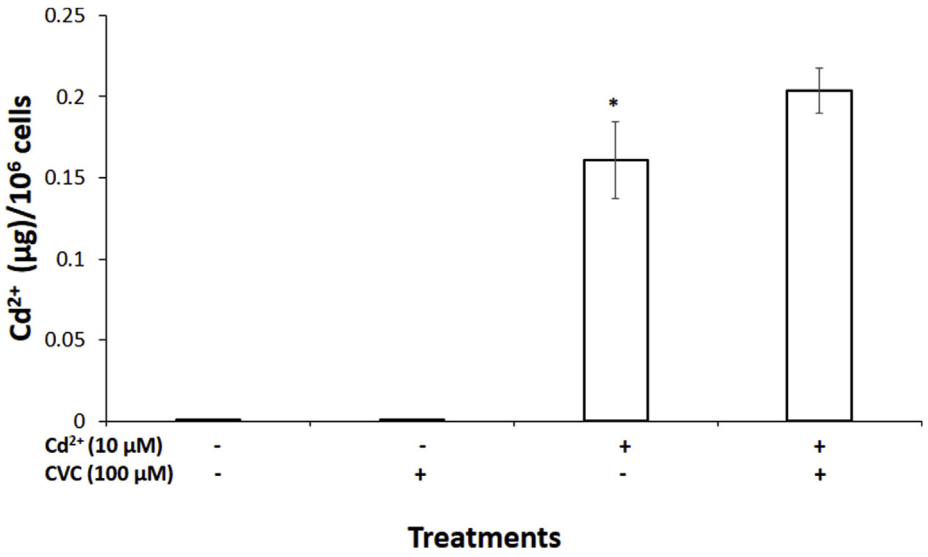

Fig. 10. Effects of CVC on Cd^{2+} uptake in PC12 cells exposed/co-exposed with 10 µM Cd^{2+} and 100 µM CVC for 48 h, measured by using ICP-MS analysis. Error bars indicate mean ± S.E.M. (n = 3), * and # indicate significant differences (P < 0.05) from the control group and the Cd^{2+}-exposed group, respectively.

(Fig. 1B) and increased the level of LDH activity in culture media (Fig. 2). These effects were reversed by the action of CVC (100 µM) after co-exposure. Here, it has been indicated that CVC (100 µM) can reduce the cell death by alleviating oxidative stress exerted by Cd^{2+} (10 µM). The oxidative stress ameliorating activity of CVC found in our research can be supported by previous findings. For instance, a recent study showed that CVC reduces oxidative stress by increasing the GSH levels against paracetamol-induced toxicity in HepG2 cells (Palabiyik et al., 2016).

Cd^{2+} exposure induces apoptosis in a number of cell systems including PC12 cells (Rahman et al., 2017). The flow cytometry analyses in our study showed that CVC (100 µM) when co-exposed with Cd^{2+} (10 µM), recovered more than half of the apoptotic PC12 cells (from > 54% to about 26%) compared to only Cd^{2+} (10 µM) exposure (Fig. 5). One of the probable reasons behind this performance to rescue cells from apoptosis is the ameliorating effects of CVC (100 µM) on oxidative stress posed by Cd^{2+} (10 µM). CVC also contributed to the inhibitory effect against oxidative DNA damage, as well as enhancing effect on the cell cycle progression, through inducing antioxidant protection. Previous studies have reported that Cd^{2+} exposure accelerates the ROS induced DNA damages, inhibits the repair of oxidative DNA damage, affects cell cycle progression and induces apoptosis in various cell lines (e.g., HepG2 cells) (Rani et al., 2014; Skipper et al., 2016; Norbury and Zhivotovsky, 2004). In a recent study, Horvathova et al. (2007) established the inhibitory effects of CVC on H_2O_2 induced DNA damage in K562 cells. We measured the intact DNA density following agarose gel electrophoresis and a considerable amount of intact DNA was fragmented by exposure to Cd^{2+} (10 µM). However, exposure to combined Cd^{2+} (10 µM) and CVC (100 µM) increased the amount of intact DNA significantly (Fig. 4A and B), thereby minimizing the DNA damage.

It has already been established that a leucine zipper transcription factor namely Nrf2 mediates an important signaling pathway leading to cellular protection against oxidative stress and electrophilic compounds (Loboda et al., 2016). Normally, Nrf2 is sequestered in a complex with kelch-like ECH-associated protein 1 (Keap1) in the cytoplasm. But, onset of oxidative stress disassociates and translocates Nrf2 into the nucleus to bind with antioxidant responsive element (ARE). This binding allows expressions of cytoprotective genes such as *HMOX1* and *NQO1* (Zhang et al., 2017; Taguchi et al., 2011). Even though the

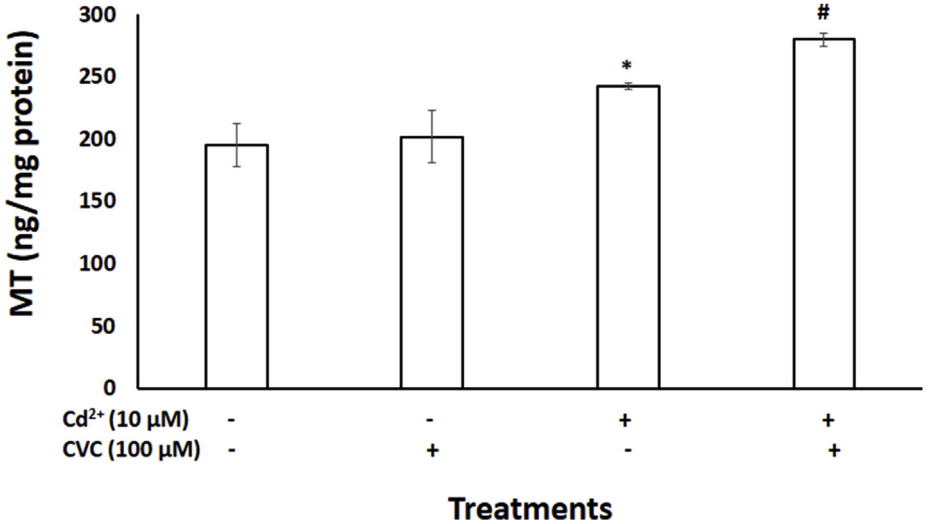

Fig. 11. Effects of CVC on metallothionein (MT) content in PC12 cells exposed/co-exposed with 10 µM Cd^{2+} and 100 µM CVC for 48 h, determined by ELISA. Error bars indicate mean ± S.E.M. (n = 3), * and # indicate significant differences (P < 0.05) from the control group and the Cd^{2+}-exposed group, respectively.

underlying molecular mechanism is still unclear, the inactivation of Nrf2 is necessary for the accomplishment of apoptosis (Méndez-García et al., 2019). In the current research, we found that upon co-exposure CVC (100 μM) significantly lessened the Cd^{2+}-imposed inactivation of Nrf2 (Fig. 7A and B) and perhaps promoted the expressions of antioxidant enzymes. Additionally, the involvement of a variety of oxidative transcription factors like NFκB is responsible for achieving Cd^{2+}-induced apoptosis. It has been suggested that apoptosis due to Cd^{2+} toxicity in rat kidney proximal tubular epithelial cells, NRK-52E, involves the down regulation of NFκB which could facilitated oxidative stress (Xie and Shaikh, 2006). Oxidative stress also inhibits autophagy related pro-survival proteins like mTOR and Akt in the PI3/mTOR/Akt signaling pathway leading to the induction of Bax expression and suppression of Bcl-2 which ultimately activates caspase cascade to induce apoptosis (Rahman et al., 2018; Roy et al., 2014; Singh et al., 2012). As shown in Fig. 6A and B, Cd^{2+} (10 μM) induced down-regulated expressions of NFκB, mTOR and Akt, which were considerably increased by the co-exposure of Cd^{2+} (10 μM) and CVC (100 μM). Furthermore, the involvement of MAPKs pathways has already been elucidated in various cell lines undergoing *in vitro* apoptotic as well as necrotic cell death induced by Cd^{2+}. ERK1 belongs to MAPKs protein family which is known to be involved in cell proliferation, differentiation, and apoptosis. A contemporary research by Hu et al. (2015) has shown that Cd^{2+} encourages apoptosis in MG63 cells by increasing ROS and inhibiting ERK 1/2 pathway. Our results also exhibited a significant down regulation of ERK1 by Cd^{2+} toxicity which was meaningfully recovered by combined exposure with CVC (100 μM) (Fig. 7A and B). Again, the probable reason for ERK1 revival is that CVC could ameliorate the oxidative stress and placate the ROS activity.

Cd^{2+} encourages mitochondrial permeability transition pore (MPTP) opening, facilitates the release of apoptogenic proteins into the cytosol and thus intensifies the occurrence of multiple apoptotic pathways via caspase-dependent (releasing cytochrome *c*) or via caspase-independent (releasing AIF and Endo G) pathways. However, the activation of mitochondrial apoptotic pathways largely contributes to the manifestation of apoptotic death caused by Cd^{2+} toxicity (Liu et al., 2016b). Cumulative evidences from studies on a number of cell lines suggested that the Cd^{2+}-induced oxidative stress diminishes the mitochondrial membrane potential (MMP), decreases Bcl-2/Bax ratio, releases cytochrome *c* into the cytosol, activates caspase 9, subsequently activates caspase3 and finally causes apoptosis (a process called intrinsic mitochondrial pathway) (Jiang et al., 2014; Lasfer et al., 2008). Cytochrome *c* is the most related and crucial hallmark molecule of mitochondrial apoptotic pathway; which after being released from mitochondria binds with Apaf-1 to form apoptosome and activates the caspase cascade (Choi et al., 2006). We found that Cd^{2+} (10 μM) exposure increased cytosolic cytochrome *c* level which was significantly lowered by the co-exposure of Cd^{2+} (10 μM) and CVC (100 μM) (Fig. 9A and B). Alternatively, Cd^{2+} can also induce apoptosis via extrinsic pathway. For instance, Pal et al. (2011) showed that Cd^{2+} can trigger extrinsic pathway of apoptosis by up-regulating Bid, Fas, and caspase 8 in murine hepatocytes. However, both the extrinsic and intrinsic caspase-dependent apoptotic pathways mediated by caspases 8 and 9, respectively, result in apoptosis via the cleavage and activation of the executioner caspase 3 (Wu et al., 2014). In our current research, it was depicted that Cd^{2+} (10 μM) significantly induces caspase 3 cleavage which is in accordance with the previous studies. However, this rise in cleaved caspase 3 level was considerably reduced by the co-exposure of Cd^{2+} (10 μM) and CVC (100 μM) (Fig. 8A and B). A recent finding also demonstrated that CVC provides neuroprotection on focal cerebral ischemia/reperfusion by reducing apoptosis via prohibiting caspase 3 cleavage (Yu et al., 2012). On the other hand, reports on various cell types (e.g., HEP3B cells) suggested that Cd^{2+} induces oxidative stress and subsequently releases AIF and endoG from the mitochondria into the cytosol causing caspase-independent apoptosis (Lemarié et al., 2004). Researchers also found AIF not only as an apoptotic executioner, but also as a survival protein (Sevriokova, 2011). Nevertheless, the translocation of AIF from mitochondria to the nucleus via cytosol is considered as a standard sign of caspase-independent apoptosis (Mao et al., 2011). We found a significant increase in the cytosolic AIF in PC12 cells after 48 h Cd^{2+} (10 μM) exposure which was significantly reduced by co-exposure with CVC (100 μM) (Fig. 9A and B). Therefore, it can be deduced from our findings that CVC can ameliorate both caspase-dependent and caspase-independent apoptosis upon Cd^{2+}-induced oxidative stress.

MTs are divalent, cysteine-rich small metal-binding stress-proteins ubiquitously expressed in many tissues; but expressions are induced by a variety of factors especially by metal ions such as Cd^{2+}. It was recommended that cells synthesizing MTs are resistant, while cells not synthesizing MTs are sensitive to Cd^{2+} toxicity. It also have been

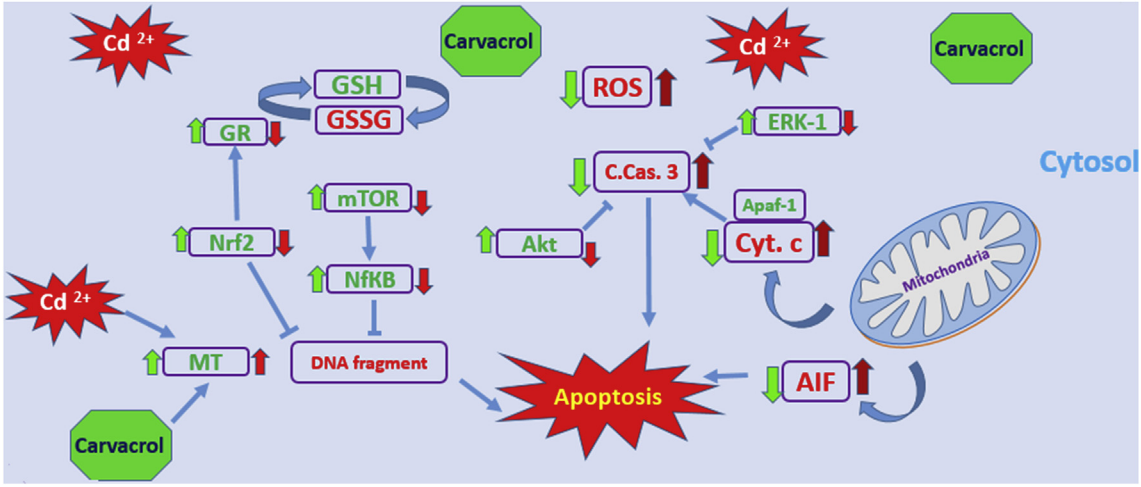

Fig. 12. A schematic representation of the proposed molecular mechanism of cytoprotective and survival-enhancing effects of CVC against Cd^{2+}-triggered oxidative stress and caspase dependent/independent apoptosis in PC12 cells. Red arrows = effects of Cd^{2+}; green arrows = effects of CVC, CVC reduces Cd2+ toxicity by GR expression and thus enhancing the conversion of GSSG to GSH indicating the lowered occurrence of ROS. It also up-regulates the Cd^{2+}-induced down-regulated expressions of mTOR, NFκB and Nrf2. CVC increases the expressions of Akt and ERK1 and suppresses the cleavage of caspase 3 producing less amount of c. caspase 3. Cytosolic releases of Cyt. c and AIF from mitochondria are also prohibited by CVC. Moreover, CVC reduces the DNA fragmentation and increases MT expression. The combined effect of the above phenomena exerted by CVC is the amelioration of Cd^{2+}-induced oxidative stress and caspase dependent/independent apoptosis in PC12 cells. (For interpretation of the references to colour in this figure legend, the reader is referred to the Web version of this article.)

reported that MTs protect cells from oxidative species reacting with sulfhydryl groups (Ruttkay-Nedecky et al., 2013). Although the physiological functions of MTs are still debated, a number of *in vivo* studies showed that MTs are induced in tissues upon Cd^{2+} exposure and is engaged in the metabolism and detoxification through Cd^{2+} binding (Lu et al., 2001). Likewise, a recent *in vitro* study on HEK293 cell system demonstrated that MTs overexpression protected cells against Cd^{2+} (10 μM) toxicity (Li et al., 2005). Similarly, we found that the MTs were considerably overexpressed in PC12 cells after exposure to Cd^{2+} (10 μM) (Fig. 11). Surprisingly, we also observed that the MTs expression level was significantly higher in cells co-exposed to Cd^{2+} (10 μM) and CVC (100 μM) in comparison to that of the Cd^{2+} (10 μM) exposed cells. A previous study supported our finding showing that CVC can boost the overexpression of MTs in tolerogenic dendritic cells (Spiering et al., 2012). Therefore, the higher uptake of Cd^{2+} (Fig. 10) by PC12 cells co-exposed with Cd^{2+} (10 μM) and CVC (100 μM) might be explained by the overexpression of MT and probable increase in Cd^{2+}-binding by MTs.

Overall, we summarized that CVC protected PC12 cells from Cd^{2+}-triggered toxicity by combating oxidative stress, increasing GSH levels, upregulating GR-expression, and reducing DNA damage; as well as, stimulating ERK-1 MAPK expression, activating expressions of Nrf2,NFκB and autophagy related pro-survival proteins-mTOR and Akt, and promoting MT overexpression(Fig. 12). Moreover, CVC effectively defended cells against both Cd^{2+}-induced caspase-dependent and caspase-independent apoptosis through hindering caspase 3 cleavage, and prohibiting cytochrome *c* and AIF release into cytosol from mitochondria.

Therefore, it became certain that the natural antioxidant, CVC acted as a powerful anti-oxidative and anti-apoptotic agent against Cd^{2+} in PC12 cells. Finally, we recommend CVC as a potential and safe therapeutic agent against the toxicity posed by the toxic heavy metal, Cd^{2+}, in the biological system. However, further *in vivo* and *in vitro* researches are required for precise understanding of the effects, interactions and mechanism(s) of action of CVC against cadmium-induced toxicity. To add, investigations are also necessary to understand the outcome of CVC treatment on other metal or non-metal toxicants in a diverse array of biological systems.

Declaration of competing interest

The authors declare that they have no known competing financial interests or personal relationships that could have appeared to influence the work reported in this paper.

Appendix A. Supplementary data

Supplementary data to this article can be found online at https://doi.org/10.1016/j.fct.2019.110835.

References

Aeschbach, R., Löliger, J., Scott, B.C., Murcia, A., Butler, J., Halliwell, B., Aruoma, O.I., 1994. Antioxidant actions of thymol, carvacrol, 6-gingerol, zingerone and hydroxytyrosol. Food Chem. Toxicol. 32, 31–36. https://doi.org/10.1016/0278-6915(84)90033-4.

Aristatile, B., Al-Numair, K.S., Veeramani, C., Pugalendi, K.V., 2009. Effect of carvacrol on hepatic marker enzymes and antioxidant status in D-galactosamine-induced hepatotoxicity in rats. Fundam. Clin. Pharmacol. 23, 757–765. https://doi.org/10.1111/j.1472-8206.2009.00721.x.

Badisa, V.L.D., Latinwo, L.M., Odewumi, C.O., Badisa, R.B., Ayuk-Takem, L.T., Nwoga, J., West, J., 2007. Mechanism of DNA damage by cadmium and interplay of antioxidant enzymes and agents. Environ. Toxicol. 22, 144–151. https://doi.org/10.1002/tox.20248.

Beena, Kumar, D., Rawat, D.S., 2013. Synthesis and antioxidant activity of thymol and carvacrol based Schiff bases. Bioorg. Med. Chem. Lett 23, 641–645. https://doi.org/10.1016/j.bmcl.2012.12.001.

Chatterjee, S., Kundu, S., Sengupta, S., Bhattacharyya, A., 2009. Divergence to apoptosis from ROS induced cell cycle arrest: effect of cadmium. Mutat. Res. 663, 22–31. https://doi.org/10.1016/j.mrfmmm.2008.12.011.

Choi, Y.K., Kim, T.K., Kim, C.J., Lee, J.S., Oh, S.Y., Joo, H.S., Foster, D.N., Hong, K.C., You, S., Kim, H., 2006. Activation of the intrinsic mitochondrial apoptotic pathway in swine influenza-mediated cell death. Exp. Mol. Med. 38, 11–17. https://www.nature.com/articles/emm20062.

Cui, Z., Xie, Z., Wang, B., Zhong, B., Chen, X., Sun, Y., Sun, Q., Yang, G., Bian, L., 2015. Carvacrol protects neuroblastoma SH-SY5Y cells against Fe^{2+} -induced apoptosis by suppressing activation of MAPK/JNK-NF-κB signaling pathway. Acta Pharmacol. Sin. 36, 1426–1436. https://doi.org/10.1038/aps.2015.90.

Du, Z.X., Zhang, H.Y., Meng, X., Guan, Y., Wang, H.Q., 2009. Role of oxidative stress and intracellular glutathione in the sensitivity to apoptosis induced by proteasome inhibitor in thyroid cancer cells. BMC Canc. 9, 56. https://doi.org/10.1186/1471-2407-9-56.

Dudley, R.E., Svoboda, D.J., Klaassen, C.D., 1982. Acute exposure to cadmium caused severe liver injury in rats. Toxicol. Appl. Pharmacol. 65, 302–313. https://doi.org/10.1016/0041-008X(82)90013-8.

Horvathova, E., Turcaniova, V., Slamenova, D., 2007. Comparative study of DNA-damaging and DNA-protective effects of selected components of essential plant oils in human leukemic cells K562. Neoplasma 54, 478–483.

Hu, K.-H., Li, W.X., Sun, M.Y., Zhang, S.B., Fan, C.X., Wu, Q., Zhu, W., Xu, X., 2015. Cadmium induced apoptosis in MG63 cells by increasing ROS, activation p38 MAPK and inhibition of ERK 1/2 pathways. Cell. Physiol. Biochem. 36, 642–654. https://doi.org/10.1159/000430127.

Ikediobi, C.O., Badisa, V.L., Ayuk-Takem, L.T., Latinwo, L.M., West, J., 2004. Response of antioxidant enzymes and redox metabolites to cadmium-induced oxidative stress in CRL-1439 normal rat liver cells. Int. J. Mol. Med. 14, 87–92. https://doi.org/10.3892/ijmm.14.1.87.

James, K.A., Meliker, J.R., 2013. Environmental cadmium exposure and osteoporosis: a review. Int. J. Public Health 58, 737–745. https://doi.org/10.1007/s00038-013-0488-8.

Järup, L., Åkesson, A., 2009. Current status of cadmium as an environmental health problem. Toxicol. Appl. Pharmacol. 238, 201–208. https://doi.org/10.1016/j.taap.2009.04.020.

Jiang, C., Yuan, Y., Hu, F., Wang, Q., Zhang, K., Wang, Y., Gu, J., Liu, X., Bian, J., Liu, Z., 2014. Cadmium induces PC12 cells apoptosis via an extracellular signal-regulated kinase and c-jun N-terminal kinase-mediated mitochondrial apoptotic pathway. Biol. Trace Elem. Res. 158, 249–258. https://doi.org/10.1007/s12011-014-9918-6.

Karkabounas, S., Kostoula, O.K., Daskalou, T.A., Veltsistas, P., Karamouzis, M.V., Zelovitis, I., Metsios, M.K., Lekkas, P., Evangelou, A.M., Kotsis, N., Skoufos, I., 2006. Anticarcinogenic and antiplatelet effects of carvacrol. Exp. Oncol. 28, 121–125.

Kerkhove, E.V., Pennemans, V., Swennen, Q., 2010. Cadmium and transport of ions and substances across cell membranes and epithelia. Biometals 23, 823–855. https://doi.org/10.1007/s10534-010-9357-6.

Kihara, Y., Yustiawati, Tanaka, M., Gumiri, S., Ardianor, Hosokawa, T., Tanaka, S., Saito, T., Kurasaki, M., 2012. Mechanism of the toxicity induced by natural humic acid on human vascular endothelial cells. Environ. Toxicol. 29, 916–925. https://doi.org/10.1002/tox.21829.

Kirimer, N., Başer, K.H.C., Tümen, G., 1995. Carvacrol rich plants in Turkey. Chem. Nat. Compd. 31, 37–41. https://doi.org/10.1007/BF01167568.

Landa, P., Kokoska, L., Pribylova, M., Vanek, T., Marsik, P., 2009. In vitro anti-inflammatory activity of carvacrol: inhibitory effect on COX-2 catalyzed prostaglandin E_2 biosynthesis. Arch Pharm. Res. 32, 75–78. https://doi.org/10.1007/s12272-009-1120-6.

Lasfer, M., Vadrot, N., Aoudjehane, L., Conti, F., Bringuier, A.F., Feldmann, G., Reyl-Desmars, F., 2008. Cadmium induces mitochondria-dependent apoptosis of normal human hepatocytes. Cell Biol. Toxicol. 24, 55–62. https://doi.org/10.1007/s10565-007-9015-0.

Lemarié, A., Lagadic-Gossmann, D., Morzadec, C., Allain, N., Fardel, O., Vernhet, L., 2004. Cadmium induces caspase-independent apoptosis in liver HEP3B cells: role for calcium in signaling oxidative stress-related impairment of mitochondria and relocation of endonuclease G and apoptosis inducing factor. Free Radic. Biol. Med. 36, 1517–1531. https://doi.org/10.1016/j.freeradbiomed.2004.03.020.

Li, J., Liu, Y., Ru, B., 2005. Effect of metallothionein on cell viability and its interactions with cadmium and zinc in HEK293 cells. Cell Biol. Int. 29, 843–848. https://doi.org/10.1016/j.cellbi.2005.05.008.

Liu, G., Zou, H., Lou, T., Long, M., Bian, J., Liu, X., Gu, J., Yuan, Y., Song, R., Wang, Y., Zhu, J., Liu, Z., 2016b. Caspase-dependent and caspase-independent pathways are involved in cadmium-induced apoptosis in primary rat proximal tubular cell culture. PLoS One 11, e0166823. https://doi.org/10.1371/journal.pone.0166823.

Liu, X., Zhang, Y., Wang, Y., Yan, Y., Wang, J., Gu, J., Chun, B., Liu, Z., 2016a. Investigation of cadmium-induced apoptosis and the protective effect of N-acetylcysteine in BRL 3A cells. Mol. Med. Rep. 14, 373–379. https://doi.org/10.3892/mmr.2016.5218.

Liu, Y., Templeton, D.M., 2008. Initiation of caspase-independent death in mouse mesangial cells by Cd^{2+}: involvement of p38 kinase and CaMK-II. J. Cell. Physiol. 217, 307–318. https://doi.org/10.1002/jcp.21499.

Loboda, A., Damulewicz, M., Pyza, E., Jozkowicz, A., Dulak, J., 2016. Role of Nrf2/HO-1 system in development, oxidative stress response and diseases: an evolutionarily conserved mechanism. Cell. Mol. Life Sci. 73, 3221–3247. https://doi.org/10.1007/s00018-016-2223-0.

Lu, J., Jin, T., Nordberg, G., Nordberg, M., 2001. Metallothionein gene expression in peripheral lymphocytes from cadmium-exposed workers. Cell Stress Chaperones 6, 97–104.

Mao, W.P., Zhang, N.N., Zhou, F.Y., Li, W.X., Liu, H.Y., Feng, J., Zhou, L., Wei, C.J., Pan, Y.B., He, Z.J., 2011. Cadmium directly induced mitochondrial dysfunction of human embryonic kidney cells. Hum. Exp. Toxicol. 30, 920–929. https://doi.org/10.1177/0960327110384286.

Méndez-García, L.A., Martínez-Castillo, M., Villegas-Sepúlveda, N., Orozco, L., Córdova, E.J., 2019. Curcumin induces p53-independent inactivation of Nrf2 during oxidative stress-induced apoptosis. Hum. Exp. Toxicol. 24https://doi.org/10.1177/0960327119845035. 960327119845035.

Nemmiche, S., 2017. Oxidative signaling response to cadmium exposure. Toxicol. Sci. 156, 4–10. https://doi.org/10.1093/toxsci/kfw222.

Nishijo, M., Morikawa, Y., Nakagawa, H., Tawara, K., Miura, K., Kido, T., Ikawa, A., Kobayashi, E., Nogawa, K., 2006. Causes of death and renal tubular dysfunction in residents exposed to cadmium in the environment. Occup. Environ. Med. 63, 545–550. https://doi.org/10.1136/oem.2006.026591.

Norbury, C.J., Zhivotovsky, B., 2004. DNA damage-induced apoptosis. Oncogene 23, 2797–2808.

Noshy, P.A., Elhady, M.A., Khalaf, A.A.A., Kamel, M.M., Hassanen, E.I., 2018. Ameliorative effect of carvacrol against propiconazole-induced neurobehavioral toxicity in rats. Neurotoxicology 67, 141–149. https://doi.org/10.1016/j.neuro.2018.05.005.

Oh, S.H., Lim, S.C., 2006. A rapid and transient ROS generation by cadmium triggers apoptosis via caspase-dependent pathway in HepG2 cells and this is inhibited through N-acetylcysteine-mediated catalase upregulation. Toxicol. Appl. Pharmacol. 212, 212–223. https://doi.org/10.1016/j.taap.2005.07.018.

Pal, S., Pal, P.B., Das, J., Sil, P.C., 2011. Involvement of both intrinsic and extrinsic pathways in hepatoprotection of arjunolic acid against cadmium induced acute damage in vitro. Toxicology 283, 129–139. https://doi.org/10.1016/j.tox.2011.03.006.

Palabiyik, S., Karakus, E., Halici, Z., Cadirci, E., Bayir, Y., Ayaz, G., Cinar, I., 2016. The protective effects of carvacrol and thymol against paracetamol-induced toxicity on human hepatocellular carcinoma cell lines (HepG2). Hum. Exp. Toxicol. 35, 1252–1263. https://doi.org/10.1177/0960327115627688.

Patra, R.C., Rautray, A.K., Swarup, D., 2011. Oxidative stress in lead and cadmium and its amelioration. Vet. Med. Int. 457327. https://doi.org/10.4061/2011/457327.

Rahman, M.M., Lopez-Uson, A.R., Sikder, M.T., Tan, G., Hosokawa, T., Saito, T., Kurasaki, M., 2018. Ameliorative effects of selenium on arsenic-induced cytotoxicity in PC12 cells via modulating autophagy/apoptosis. Chemosphere 196, 453–466. https://doi.org/10.1016/j.chemosphere.2017.12.149.

Rahman, M.M., Ukiana, J., Lopez, R.U., Sikder, M.T., Saito, T., Kurasaki, M., 2017. Cytotoxic effects of cadmium and zinc co-exposure in PC12 cells and the underlying mechanism. Chem. Biol. Interact. 269, 41–49. https://doi.org/10.1016/j.cbi.2017.04.003.

Ramos, M., Jiménez, A., Garrigós, M.C., 2016. Carvacrol-based films: usage and potential in antimicrobial packaging. In: Barros-Velázquez, J. (Ed.), Antimicrobial Food Packaging. Academic Press, pp. 329–338. https://doi.org/10.1016/B978-0-12-800723-5.00026-7.

Rani, A., Kumar, A., Lal, A., Pant, M., 2014. Cellular mechanisms of cadmium-induced toxicity: a review. Int. J. Environ. Health Res. 24, 378–399. https://doi.org/10.1080/09603123.2013.835032.

Roos, W.P., Kaina, B., 2006. DNA damage-induced cell death by apoptosis. Trends Mol. Med. 12, 440–450. https://doi.org/10.1016/j.molmed.2006.07.007.

Roy, R., Singh, S.K., Chauhand, L.K.S., Das, M., Tripathi, A., Dwivedi, P.D., 2014. Zinc oxide nanoparticles induce apoptosis by enhancement of autophagy via PI3K/Akt/mTOR inhibition. Toxicol. Lett. 227, 29–40. https://doi.org/10.1016/j.toxlet.2014.02.024.

Ruttkay-Nedecky, B., Nejdl, L., Gumulec, J., Zitka, O., Masarik, M., Eckschlager, T., Stiborova, M., Adam, V., Kizek, R., 2013. The role of metallothionein in oxidative stress. Int. J. Mol. Sci. 14, 6044–6066. https://doi.org/10.3390/ijms14036044.

Samarghandian, S., Farkhondeh, T., Samini, F., Borji, A., 2016. Protective effects of carvacrol against oxidative stress induced by chronic stress in rat's brain, liver and kidney. Biochem. Res. Int. 2645237. https://dx.doi.org/10.1155/2016/2645237.

Sarkar, S., Yadav, P., Bhatnagar, D., 1998. Lipid peroxidative damage on cadmium exposure and alterations in antioxidant system in rat erythrocytes: a study with relation to time. Biometals 11, 153–157. https://doi.org/10.1023/A:1009286130324.

Sevriokova, I.F., 2011. Apoptosis-inducing factor: structure, function and redox regulation. Antioxidants Redox Signal. 14, 2545–2579. https://doi.org/10.1089/ars.2010.3445.

Singh, B.N., Kumar, D., Shankar, S., Srivastava, R.K., 2012. Rottlerin induces autophagy which leads to apoptotic cell death through inhibition of PI3/Akt/mTOR pathway in human pancreatic cancer stem cell. Biochem. Pharmacol. 84, 1154–1163. https://doi.org/10.1016/j.bcp.2012.08.007.

Skipper, A., Sims, J.N., Yedjou, C.G., Tchounwou, P.B., 2016. Cadmium chloride induces DNA damage and apoptosis of human liver carcinoma cells via oxidative stress. Int. J. Environ. Res. Public Health 13, 88. https://doi.org/10.3390/ijerph13010088.

Spiering, R., Zee, R.V.D., Wagenaar, J., Kapetis, D., Zolezzi, F., Eden, W.V., Broer, F., 2012. Tolerogenic Dendritic cells that inhibit autoimmune arthritis can be induced by a combination of carvacrol and thermal stress. PLoS One 7, e46336. https://doi.org/10.1371/journal.pone.0046336.

Stohs, S.J., Bagchi, D., Hassoun, E., Bagchi, M., 2000. Oxidative mechanisms in the toxicity of chromium and cadmium ions. J. Environ. Pathol. Toxicol. Oncol. 19, 201–213. https://doi.org/10.1615/JEnvironPatholToxicolOncol.v20.i2.10.

Taguchi, K., Motohashi, H., Yamamoto, M., 2011. Molecular mechanisms of the Keap1-Nrf2 pathway in stress response and cancer evolution. Genes Cells 16, 123–140. https://doi.org/10.1111/j.1365-2443.2010.01473.x.

Tellez-Plaza, M., Jones, M.R., Dominguez-Lucas, A., Guallar, E., Navas-Acien, A., 2013. Cadmium exposure and clinical cardiovascular disease: a systematic review. Curr. Atheroscler. Rep. 15, 356–371. https://doi.org/10.1007/s11883-013-0356-2.

Templeton, D.M., Liu, Y., 2010. Multiple roles of cadmium in cell death and survival. Chem. Biol. Interact. 188, 267–275. https://doi.org/10.1016/j.cbi.2010.03.040.

Wang, B., Du, Y., 2013. Cadmium and its neurotoxic effects. Oxid. Med. Cell Longev. 898034. https://doi.org/10.1155/2013/898034.

Wang, P., Luo, Q., Qiao, H., Ding, H., Cao, Y., Yu, J., Liu, R., Zhang, Q., Zhu, H., Qu, L., 2017. The neuroprotective effects of carvacrol on ethanol-induced hippocampal neurons impairment via the antioxidative and antiapoptotic pathways. Oxid. Med. Cell Longev. 4079425. https://doi.org/10.1155/2017/4079425.

Wu, M.-H., Jin, X.-K., Yu, A.-Q., Zhu, Y.-T., Li, D., Li, W.-W., Wang, Q., 2014. Caspase-mediated apoptosis in crustaceans: cloning and functional characterization of EsCaspase-3-like protein from *Eriocheir sinensis*. Fish Shellfish Immunol. 41, 625–632. https://doi.org/10.1016/j.fsi.2014.10.017.

Xie, J., Shaikh, Z.A., 2006. Cadmium-induced apoptosis in rat kidney epithelial cells involves decrease in nuclear factor-kappa B activity. Toxicol. Sci. 91, 299–308. https://doi.org/10.1093/toxsci/kfj131.

Xu, J., Zhou, F., Ji, B.-P., Pei, R.-S., Vu, N., 2008. The antibacterial mechanism of carvacrol and thymol against Escherichia coli. Lett. Appl. Microbiol. 47, 174–179. https://doi.org/10.1111/j.1472-765X.2008.02407.x.

Yu, H., Zhang, Z.-L., Chen, J., Pei, A., Hua, F., Qian, X., He, J., Liu, C.-F., Xu, X., 2012. Carvacrol, a food-additive, provides neuroprotection on focal cerebral ischemia/reperfusion injury in mice. PLoS One 7, e33584. https://doi.org/10.1371/journal.pone.0033584.

Zhang, C., Lin, J., Ge, J., Wang, L.L., Li, N., Sun, X.T., Cao, J.L., 2017. Selenium triggers Nrf2-mediated protection against cadmium-induced chicken hepatocyte autophagy and apoptosis. Toxicol. In Vitro 44, 349–356. https://doi.org/10.1016/j.tiv.2017.07.027.

Zhou, Y., Zhang, S., Liu, C., Cai, Y., 2009. The protection on ROS mediated-apoptosis by mitochondria dysfunction in cadmium-induced LLC-PK_1 cells. Toxicol. In Vitro 23, 288–294. https://doi.org/10.1016/j.tiv.2008.12.009.

Zotti, M., Colaianna, M., Morgese, M.G., Tucci, P., Schiavone, S., Avato, P., Trabace, L., 2013. Carvacrol: from ancient flavoring to neuromodulatory agent. Molecules 18, 6161–6172. https://doi.org/10.3390/molecules18066161.